Acta Cryst E CRYSTALLOGRAPHIC COMMUNICATIONS

ISSN 2056-9890

Crystal structure and Hirshfeld surface analysis of 5-bromo-1,3,4-thiadiazol-2-amine

Batirbay Torambetov,[a] Miyribek Djiemuratov,[a] Abdusamat Rasulov,[b] Mehmet Akkurt,[c] Gizachew Mulugeta Manahelohe,[d]* Khudayar I. Hasanov[e] and Punhan J. Jamalov[f]

[a]National University of Uzbekistan named after Mirzo Ulugbek, 4 University St., Tashkent, 100174, Uzbekistan, [b]Termez University of Economics and Service, 41B Farovon St., Termiz, 190111, Uzbekistan, [c]Department of Physics, Faculty of Sciences, Erciyes University, 38039 Kayseri, Türkiye, [d]Department of Chemistry, University of Gondar, PO Box 196, Gondar, Ethiopia, [e]Azerbaijan Medical University, Scientific Research Centre (SRC), A. Kasumzade St. 14, AZ 1022, Baku, Azerbaijan, and [f]Department of Chemical Engineering, Baku Engineering University, Khirdalan, Hasan Aliyev str. 120, AZ0101, Absheron, Azerbaijan. *Correspondence e-mail: Gizachew.Mulugeta@uog.edu.et

Received 6 May 2026
Accepted 20 May 2026

Edited by C. Schulzke, Universität Greifswald, Germany

Keywords: crystal structure; hydrogen bonds; van der Waals interactions; Hirshfeld surface analysis.

CCDC reference: 2555626

Supporting information: this article has supporting information at journals.iucr.org/e

In the crystal of the title compound, $C_2H_2BrN_3S$, N—H···N hydrogen bonds connect the molecules in the form of hydrogen-bonded double-layered ribbons along the *c*-axis direction including $R_2^2(8)$ and $R_1^2(3)$ motifs, which extend to double layers in the *bc*-plane through the same hydrogen bonding albeit at different angles. The actual packing between these layers appears to also be a result of weak vdW interactions (Br/S, Br/Br) as well as Br–Br repulsion (steric and/or electrostatic). Looking along *b* or slightly deviating from that direction shows that the latter adopt a zipper pattern in order to not get too close to each other. Hirshfeld surface analysis indicates that N···H/H···N, Br···S/S···Br, Br···Br and H···H contacts account for 69.3% of the total contributions to the Hirshfeld surface.

1. Chemical context

Similar to other heterocyclic analogues, 1,3,4-thiadiazoles are widely used in medicinal, structural and coordination chemistry. In fact, the 1,3,4-thiadiazole moiety acts as a core structural component in an array of drug categories such as anticancer, analgesic, anti-inflammatory, antimicrobial, antiviral, anti-epileptic, antineoplastic, and antitubercular agents (Jain *et al.*, 2013; Torambetov *et al.*, 2026). The strong coordination ability of the nitrogen atoms is well employed in the construction/engineering of metal complexes towards functional materials (Frija *et al.*, 2016; Khojabaeva *et al.*, 2025; Mamedov *et al.*, 2006). Besides its hydrogen-bond acceptor ability, the sulfur atom of the five-membered thiadiazole ring can also behave as a chalcogen bond donor in intermolecular interactions (Gurbanov *et al.*, 2023; Mahmudov *et al.*, 2021). Thus, the presence of a sulfur atom gives it promising characteristics for the development of crystal-engineered materials (Maharramov *et al.*, 2011) as well as bioactive molecules. The design of the thiadiazol moiety with supramolecular feature facilitating sites can be used as synthetic strategy to enhance their functional properties (Huseynov *et al.*, 2021; Naghiyev *et al.*, 2023; Sadikhova *et al.*, 2024; Nuralieva *et al.*, 2025). In this work we have synthesized, isolated and structurally characterized 5-bromo-1,3,4-thiadiazol-2-amine, which exhibits various types of intermolecular interactions, both strong and weak, in its packing.

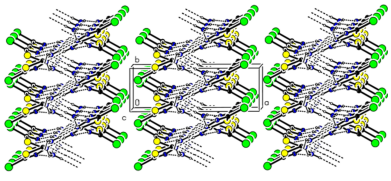

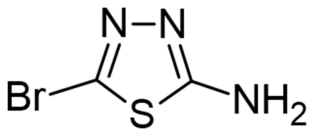

2. Structural commentary

The title molecule (Fig. 1), including the hydrogen atoms, is approximately planar with a r.m.s. deviation of fitted atoms of 0.0220 Å. The maximum deviations from the plane are 0.03 (3) Å for the N3 atom and −0.04 (6) Å and for the H3*A* atom in the opposite direction, indicative of a very subtle pyramidalization of the amine nitrogen atom N3. The values of the geometric parameters of the molecule are listed in Table 1 and they appear almost all rather normal. With regard to the C—S—C angle of 86.0 (3)°, this was presumed to be quite reasonable for thiadiazoles. However, *Mogul* (Bruno *et al.*, 2004) flagged this as an unusual case and a subsequent search of the Cambridge Structural Database (CSD, Version 6.00, last update April 2025; Groom *et al.*, 2016) with a focus on this angle was carried out for thiadiazoles where NH_2 or a halogen was present on one carbon while the substitution on the other carbon was not specified. This yielded 128 results, of which only four had similar or even more acute angles than the one in the title molecule [ZAJWAM (Makhmudov *et al.*, 2021) 86.00°; WIXFIS (Tzeng *et al.*, 1999) 85.17°; WACJIT (Pedregosa *et al.*, 1993) 85.91°; DEYNII (De Silva *et al.*, 2022) 85.98°]. The observed acute angle in the title compound is particularly notable because there is no spatial/geometric strain in the title molecule due to its comparably small substituents.

Table 1
Selected geometric parameters (Å, °).

Br1—C2	1.862 (6)	N1—N2	1.378 (7)
S1—C2	1.732 (6)	N2—C2	1.283 (7)
S1—C1	1.746 (5)	N3—C1	1.339 (8)
N1—C1	1.311 (6)		
C2—S1—C1	86.0 (3)	N3—C1—S1	122.3 (4)
C1—N1—N2	112.6 (4)	N2—C2—S1	115.4 (4)
C2—N2—N1	112.5 (5)	N2—C2—Br1	122.7 (4)
N1—C1—N3	124.1 (5)	S1—C2—Br1	121.9 (3)
N1—C1—S1	113.6 (4)		

Table 2
Hydrogen-bond geometry (Å, °).

D—H···*A*	*D*—H	H···*A*	*D*···*A*	*D*—H···*A*
N3—H3*B*···N1^{i}	0.88 (6)	2.60 (7)	3.398 (7)	150 (8)
N3—H3*A*···N1^{ii}	0.88 (6)	2.13 (6)	2.997 (7)	171 (7)
N3—H3*B*···N2^{i}	0.88 (6)	2.14 (6)	2.992 (7)	163 (6)

Symmetry codes: (i) $x, -y+\frac{1}{2}, z+\frac{1}{2}$; (ii) $-x+1, -y, -z+1$.

Table 3
Summary of short interatomic contacts (Å).

Contact	Distance	Symmetry operation
Br1···Br1	3.6914 (11)	$-x, -\frac{1}{2}+y, \frac{1}{2}-z$
S1···Br1	3.8432 (15)	$-x, 1-y, 1-z$

3. Supramolecular features

In the crystal, N—H···N hydrogen bonds connect the molecules in the form of hydrogen-bonded ribbons along the *c*-axis direction including $R_2^2(8)$ and $R_1^2(3)$ motifs (Table 2, Figs. 2 and 3). The same type of hydrogen bonds (only not in the plane of the molecules) spiral down the *b*-axis direction, forming together with the above described pattern a double layer in the *bc* plane The packing between the hydrogen-bonded layers is further likely also a matter of Br–Br repulsion (steric and/or electrostatic). When viewed along the *b*-direction direction or deviating slightly from this direction, the bromine atoms appear to form a zipper pattern while avoiding becoming too close to each other (Table 3, Fig. 4). Their Br···Br distances are, in the majority of cases, significantly longer than twice the Br vdW radius [the shortest Br–Br

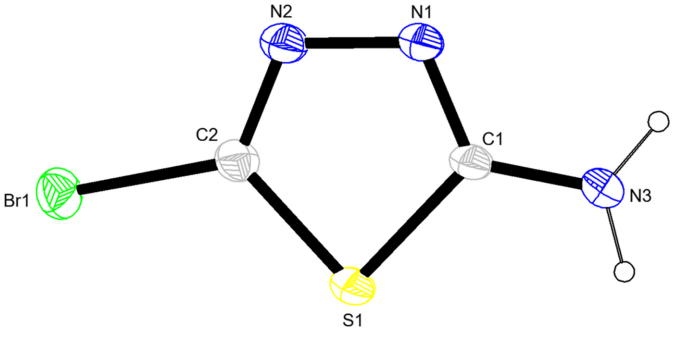

Figure 1
The title molecule with labelling scheme and displacement ellipsoids drawn at the 50% probability level.

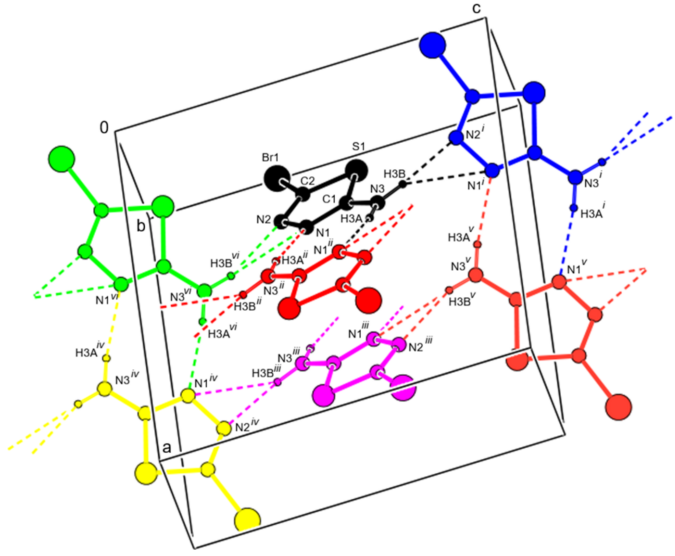

Figure 2
A general view of the intermolecular N—H···N hydrogen bonds in the unit cell. Symmetry codes: (*i*) $x, \frac{1}{2}-y, \frac{1}{2}+z$; (ii) $1-x, -y, 1-z$; (iii) $1-x, 1-y, 1-z$; (iv) $1-x, \frac{1}{2}+y, \frac{1}{2}-z$; (v) $1-x, \frac{1}{2}+y, \frac{3}{2}-z$; (vi) $x, \frac{1}{2}-y, -\frac{1}{2}+z$. Molecules with different equivalent positions are shown in different colours.

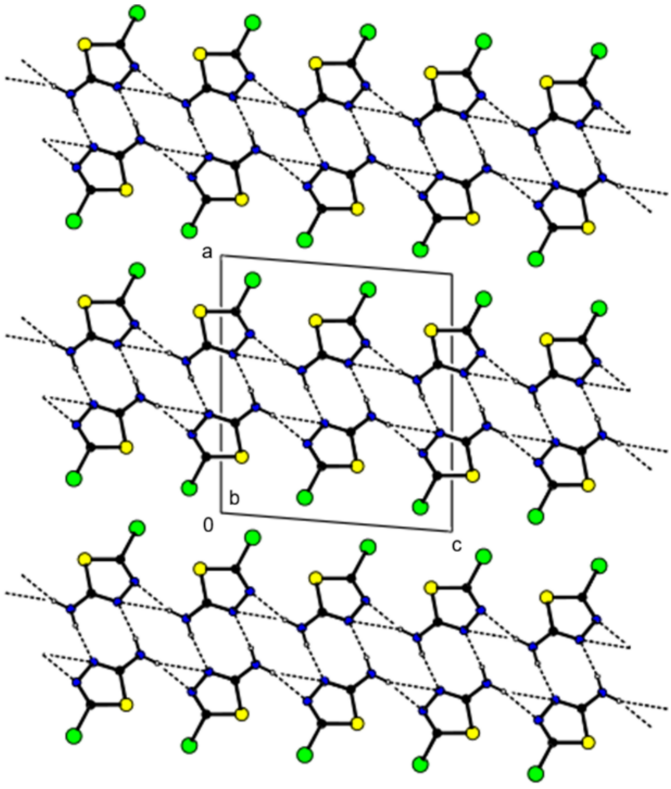

Figure 3
The ribbons connected by hydrogen bonds propagating in the [001] direction viewed along the crystallographic *b* axis. N—H···N hydrogen bonds are shown with dashed lines.

distance is 3.6914 (11) Å for each Br atom's two neighbours (see below), followed by distances of 4.034 (1) Å or longer]. The shortest distance between Br and S in the crystal is found at 3.8432 (15) Å, which is just about longer than the sum of van der Waals radii. Further, in the crystal packing there are weak or very weak Br···Br [3.6914 (11) Å, ΣrvdW(Br···Br) = 3.70Å] and S···N [3.340 (5) Å, ΣrvdW(S···N) = 3.35 Å] interactions, but if we consider experimental errors, they cannot be considered as actual halogen or chalcogen bonds, respectively. Therefore, in the crystal, with its packing pattern for interactions between the double layers, there is a balance between weak vdW attraction (S/Br and Br/Br) and Br–Br repulsion, which ultimately results in a thermodynamically

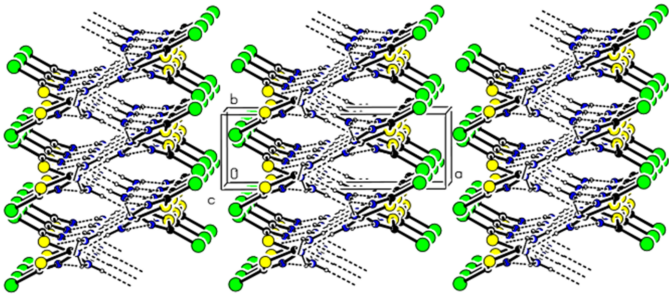

Figure 4
Packing viewed along the *c* axis with intermolecular hydrogen bonding interactions as shown in Fig. 2.

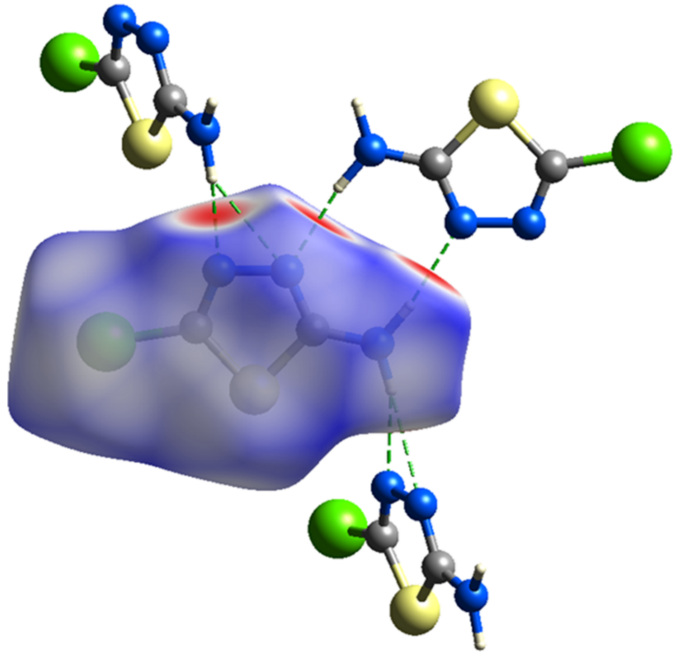

Figure 5
The title compound mapped over d_{norm} function on the Hirshfeld surface (colour code. Br: green, C: grey; H: white; N: blue; S: yellow).

stable arrangement (Tables 2 and 3). C—H···π and π–π interactions are not observed.

3.1. Hirshfeld surface analysis

A Hirshfeld surface analysis was conducted with *Crystal-Explorer* (Spackman *et al.*, 2021) to observe and quantify the intermolecular interactions in the title molecule. The Hirshfeld surfaces were mapped over d_{norm} in the range of −0.4897 (red) to +1.0166 (blue) a.u. (Fig. 5). The red regions are attributed to the N3—H3*A*···N1, N3—H3*B*···N1 and N3—H3*B*···N2 interactions (Table 2). Therefore, there is an equilibrium in the crystal between strong classical hydrogen bonding, weak van der Waals forces of attraction (S/Br and Br/Br) and repulsion (Br–Br), which ultimately leads to an energetic minimum. This is consistent with the Hirshfeld surface shown in Fig. 5, where the area around bromine is mostly blue.

The two-dimensional fingerprint plots demonstrate that the primary contributions to the crystal packing are from N···H/H···N (25.7%), Br···S/S···Br (18.1%), Br···Br (15.9%) and H···H interactions (9.6%), as shown in Fig. 6. Other less notable interactions are S···N/N···S (5.4%), Br···C/C···Br (4.4%), N···N (3.8%), N···C/C···N (3.0%), S···S (2.6%), C···C (2.5%), S···H/H···S (2.9%), S···C/C···S (2.2%), C···H/H···C (2.4%) and Br···N/N···Br (1.6%) interactions.

3.2. Crystal voids

If the molecules are closely packed and the crystals do not easily break by means of an external mechanical force, then the incorporated void volume is insignificant. The voids in the crystals of the title compound were analysed by summing up

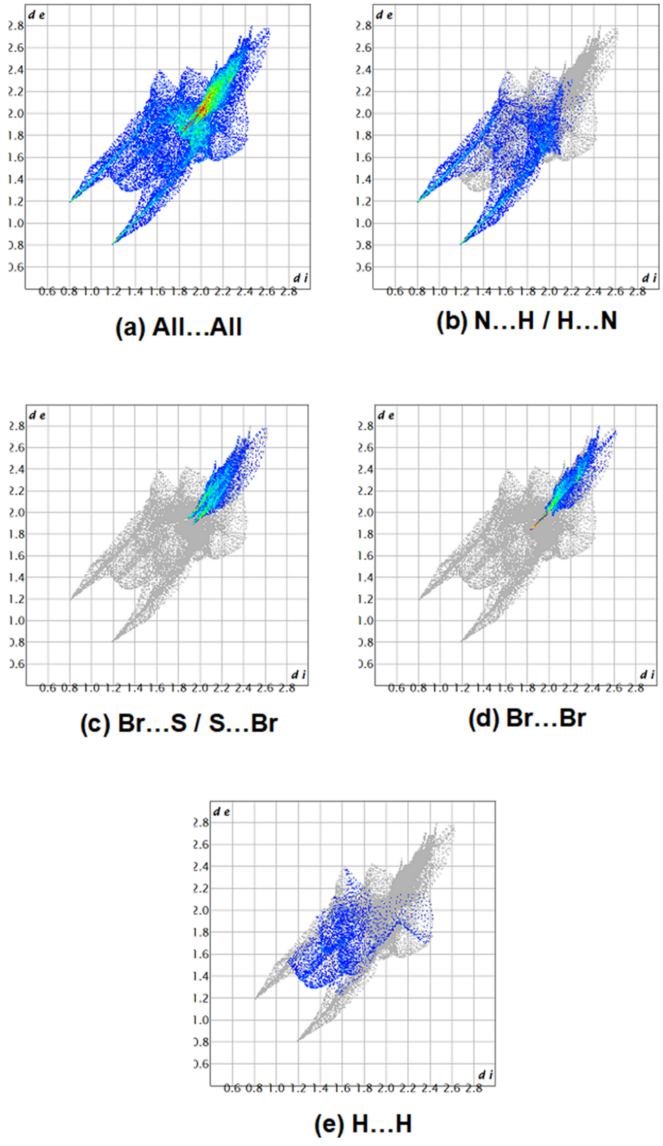

Figure 6
The two-dimensional fingerprint plots, showing (*a*) all interactions, and those delineated into (*b*) N···H/H···N, (*c*) Br···S/S···Br, (*d*) H···H interactions; d_e and d_i represent the distances from a point on the Hirshfeld surface to the nearest atoms outside (external) and inside (internal) the surface, respectively.

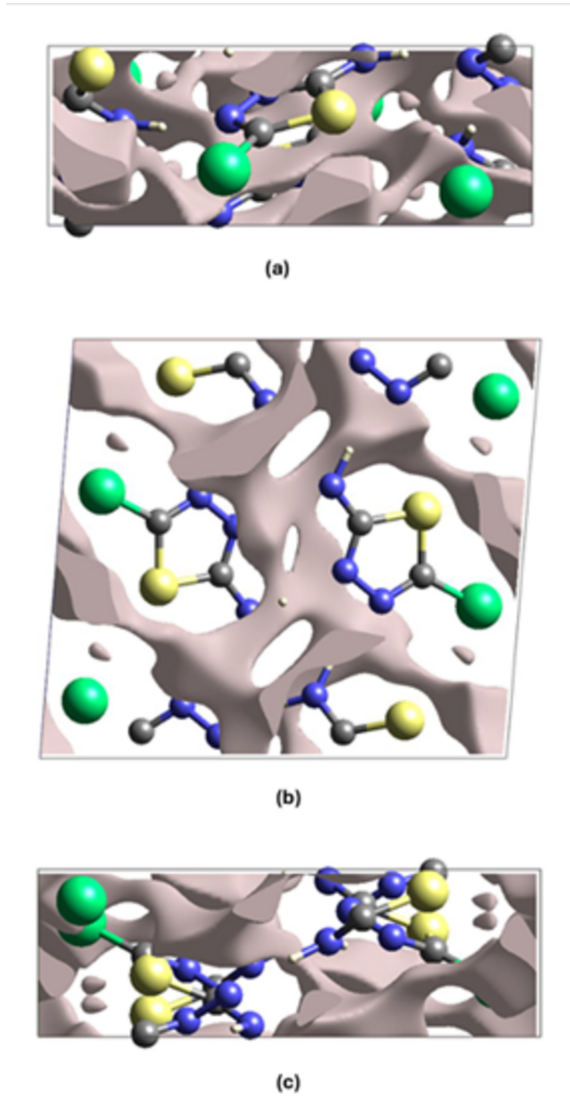

Figure 7
Graphical views of voids in the crystal packing of the title compound along the (*a*) *a*-axis, (*b*) *b*-axis and (*c*) *c*-axis directions.

the electron densities of all spherically symmetric atoms located within the unit cell (Turner *et al.*, 2011). The total volume of the crystal voids (Fig. 7) and the percentage of free space in the unit cell were calculated to be 38.37 Å^3 and 7.25%, respectively, indicating that the crystal packing is quite compact.

4. Database survey

A Cambridge Structural Database (CSD, Version 6.00, last update April 2025; Groom *et al.*, 2016) search for a thiadiazole with any halogen substituent gave only two hits (DEYMUT and DEYNII; De Silva *et al.*, 2022) emphasizing the rarity of the combination of a halogen and a thiadiazole group as in the title compound. Both of the above structures exhibit a quite notable network of intermolecular interactions. They contain bifurcated S···N as well as *X*1···*X*2 [*X*1, *X*2 = halogen (*X*1 = *X*2 = I for DEYMUT and *X*1 = I, *X*2 = Br for DEYNII)] contacts. The latter form zigzag packing patterns due to the typical angle observed in halogen bonding when the σ-hole on a halogen atom (in the two structures: Br or I) interacts with a free electron pair of a Lewis base (Metrangolo *et al.*, 2008), which in these two cases is another halogen atom (I).

Considering that the N-bound H atoms are refined relatively freely resulting in the hydrogen bonds becoming comparably short, another search was carried out for the specific hydrogen-bonding motif between the thiadiazole moieties and adjacent molecules. Excluding metals and aromatic ring structures, when searching for thiadiazoles exhibiting arrangements similar to the two shorter hydrogen-bonding motifs we observed (*i.e.*, an H···N distance range between 2.12 and 2.18 Å), we found only five hits [ESIBOA

Table 4
Experimental details.

Crystal data	
Chemical formula	$C_2H_2BrN_3S$
M_r	180.04
Crystal system, space group	Monoclinic, $P2_1/c$
Temperature (K)	293
a, b, c (Å)	12.1005 (13), 4.0336 (5), 10.8832 (14)
β (°)	94.682 (11)
V (Å^3)	529.42 (11)
Z	4
Radiation type	Cu $K\alpha$
μ (mm^{-1})	13.20
Crystal size (mm)	0.14 × 0.10 × 0.08
Data collection	
Diffractometer	XtaLAB Synergy, Single source at home/near, HyPix3000
Absorption correction	Multi-scan (*CrysAlis PRO*; Rigaku OD, 2020)
T_{min}, T_{max}	0.256, 0.348
No. of measured, independent and observed [$I > 2\sigma(I)$] reflections	3610, 1012, 915
R_{int}	0.046
(sin $\theta/\lambda)_{max}$ (Å^{-1})	0.616
Refinement	
$R[F^2 > 2\sigma(F^2)]$, $wR(F^2)$, S	0.056, 0.175, 1.15
No. of reflections	1012
No. of parameters	70
No. of restraints	1
H-atom treatment	Only H-atom coordinates refined
$\Delta\rho_{max}$, $\Delta\rho_{min}$ (e Å^{-3})	0.95, −0.97

Computer programs: *CrysAlis PRO* (Rigaku OD, 2020), *SHELXT* (Sheldrick, 2015*a*), *SHELXL* (Sheldrick, 2015*b*), *ORTEP-3 for Windows* (Farrugia, 2012) and *PLATON* (Spek, 2020).

(Slyvka *et al.*, 2021), NIYDOO02 (Dani *et al.*, 2013), VIFRUX01 (Lynch *et al.*, 2001), XUVPEK (Lynch, 2010), ZANXUJ (Köysal *et al.*, 2012)]. The respective observed pattern in the crystal of the title compound is, hence, also notably uncommon.

5. Synthesis and crystallization

To a solution of 2-amino-1,3,4-thiadiazole (5 g, 48.45 mmol) in methanol (70 mL), sodium bicarbonate (8.14 g, 96.90 mmol) and bromine (2.5 mL, 48.45 mmol) were added. The reaction mixture was stirred at room temperature until the disappearance of starting material (30–40 minutes). The methanol was removed under vacuum and the crude product was diluted with water (15 mL), filtered, and dried *in vacuo* to give a brown solid, 5-bromo-1,3,4-thiadiazol-2-amine (94%). Colourless crystals suitable for X-ray analysis were obtained by slow evaporation of ethanol solution. Analysis calculated for $C_2H_2BrN_3S$ (M = 180.02): C 13.34, H 1.12, N 23.34; found: C 13.30, H 1.10, N 23.31%. ^{1}H NMR (300 MHz, DMSO-d^6): δ 7.55 (2H). ^{13}C NMR (75 MHz, DMSO-d^6) δ 170.9 and 124.3.

6. Refinement

Crystal data, data collection and structure refinement details are summarized in Table 4. The N-bound hydrogen atoms were found in difference-Fourier maps and refined relatively freely while constrained with a SADI command at defaults and with U_{iso}(H) set to 1.2 × U_{eq}(N).

Acknowledgements

The authors' contributions are as follows; conceptualization BT, MA and GMM; synthesis, KIH and BT; X-ray analysis JA and SK; founding KIH and BT; writing (review and editing of the manuscript) BT, and MA; supervision SK, MA and GMM.

References

Bruno, I. J., Cole, J. C., Kessler, M., Luo, J., Motherwell, W. D. S., Purkis, L. H., Smith, B. R., Taylor, R., Cooper, R. I., Harris, S. E. & Orpen, A. G. (2004). *J. Chem. Inf. Comput. Sci.* **44**, 2133–2144.
Dani, R. K., Bharty, M. K., Kushawaha, S. K., Prakash, O., Singh, R. K. & Singh, N. K. (2013). *Polyhedron* **65**, 31–41.
De Silva, V., Magueres, P. L., Averkiev, B. B. & Aakeröy, C. B. (2022). *Acta Cryst.* C**78**, 716–721.
Farrugia, L. J. (2012). *J. Appl. Cryst.* **45**, 849–854.
Frija, L. M. T., Pombeiro, A. J. L. & Kopylovich, M. N. (2016). *Coord. Chem. Rev.* **308**, 32–55.
Groom, C. R., Bruno, I. J., Lightfoot, M. P. & Ward, S. C. (2016). *Acta Cryst.* B**72**, 171–179.
Gurbanov, A. V., Aliyeva, V. A., Gomila, R. M., Frontera, A., Mahmudov, K. T. & Pombeiro, A. J. (2023). *Cryst. Growth Des.* **23**, 7335–7344.
Huseynov, F. E., Mahmoudi, G., Hajiyeva, S. R., Shamilov, N. T., Zubkov, F. I., Nikitina, E. V., Prisyazhnyuk, E. D. & Kopylovich, M. N. (2021). *Polyhedron* **209**, 115453.
Jain, A. K., Sharma, S., Vaidya, A., Ravichandran, V. & Agrawal, R. K. (2013). *Chem. Biol. Drug Des.* **81**, 557–576.
Khojabaeva, G., Torambetov, B., Gonnade, R. G., Uzakbergenova, Z., Rasulov, A. & Kadirova, S. (2025). *Acta Cryst.* E**81**, 613–617.
Köysal, Y., Deniz, S., Butcher, R. J., Öztürk Yildirim, S, Jasinski, J. P. & Keeley, A. C. (2012). *Acta Cryst.* E**68**, o1279.
Lynch, D. E. (2001). *Acta Cryst.* C**57**, 1201–1203.
Lynch, D. E. (2010). Private Communication (CCDC 716834). CCDC, Cambridge, England. https://doi.org/10.5517/ccs1xpd
Maharramov, A. M., Khalilov, A. N., Sadikhova, N. D., Gurbanov, A. V. & Ng, S. W. (2011). *Acta Cryst.* E**67**, o1087.
Mahmudov, K. T., Huseynov, F. E., Aliyeva, V. A., Guedes da Silva, M. F. C. & Pombeiro, A. J. L. (2021). *Chem. Eur. J.* **27**, 14370–14389.
Makhmudov, U. S., Toshmurodov, T. T. & Ziyaev, A. A. (2021). Private Communication (CCDC 1984019). CCDC, Cambridge, England. https://doi.org/10.5517/ccdc.csd.cc24ljmx
Mamedov, S. E., Akhmedov, E. I., Kerimli, F. S. & Makhmudova, M. I. (2006). *Russ. J. Appl. Chem.* **79**, 1723–1725.
Metrangolo, P., Meyer, F., Pilati, T., Resnati, G. & Terraneo, G. (2008). *Angew. Chem. Int. Ed.* **47**, 6114–6127.
Naghiyev, F. N., Khrustalev, V. N., Akkurt, M., Khalilov, A. N., Bhattarai, A., Kerimli, F. S. & Mamedov, İ. G. (2023). *Acta Cryst.* E**79**, 494–498.
Nuralieva, G., Alieva, M., Torambetov, B., Christopher Leslee, D. B., Senthilkumar, B., Kaur, S., Dabke, N. D., Vanka, K., Ashurov, J., Kadirova, Sh. & Gonnade, R. (2025). *J. Mol. Struct.* **1338**, 142274.
Pedregosa, J. C., Alzuet, G., Borrás, J., Fustero, S., García-Granda, S. & Díaz, M. R. (1993). *Acta Cryst.* C**49**, 630–633.
Rigaku OD (2020). *CrysAlis PRO*. Oxford Diffraction Ltd, Yarnton, England.
Sadikhova, N. D., Atioğlu, Z., Guliyeva, N. A., Shelukho, E. R., Polyanskaya, D. K., Khrustalev, V. N., Akkurt, M. & Bhattarai, A. (2024). *Acta Cryst.* E**80**, 72–77.
Sheldrick, G. M. (2015*a*). *Acta Cryst.* A**71**, 3–8.
Sheldrick, G. M. (2015*b*). *Acta Cryst.* C**71**, 3–8.

Slyvka, Y., Kinzhybalo, V., Shyyka, O. & Mys'kiv, M. (2021). *Acta Cryst.* C**77**, 249–256.

Spackman, P. R., Turner, M. J., McKinnon, J. J., Wolff, S. K., Grimwood, D. J., Jayatilaka, D. & Spackman, M. A. (2021). *J. Appl. Cryst.* **54**, 1006–1011.

Spek, A. L. (2020). *Acta Cryst.* E**76**, 1–11.

Torambetov, B., Khojabaeva, G., Bharty, M. K., Gupta, S. K., Kadirova, S., Pradeep, S., Dastager, S. G. & Gonnade, R. G. (2026). *J. Mol. Struct.* **1354**, 144763.

Turner, M. J., McKinnon, J. J., Jayatilaka, D. & Spackman, M. A. (2011). *CrystEngComm* **13**, 1804–1813.

Tzeng, B.-C., Schier, A. & Schmidbaur, H. (1999). *Inorg. Chem.* **38**, 3978–3984.

supporting information

Acta Cryst. (2026). E**82**, 732-737 [https://doi.org/10.1107/S2056989026005335]

Crystal structure and Hirshfeld surface analysis of 5-bromo-1,3,4-thiadiazol-2-amine

Batirbay Torambetov, Miyribek Djiemuratov, Abdusamat Rasulov, Mehmet Akkurt, Gizachew Mulugeta Manahelohe, Khudayar I. Hasanov and Punhan J. Jamalov

Computing details

5-Bromo-1,3,4-thiadiazol-2-amine

Crystal data

$C_2H_2BrN_3S$
M_r = 180.04
Monoclinic, $P2_1/c$
a = 12.1005 (13) Å
b = 4.0336 (5) Å
c = 10.8832 (14) Å
β = 94.682 (11)°
V = 529.42 (11) Å^3
Z = 4
$F(000)$ = 344
D_x = 2.259 Mg m^{-3}
Cu $K\alpha$ radiation, λ = 1.54184 Å
Cell parameters from 2101 reflections
θ = 3.6–70.1°
μ = 13.20 mm^{-1}
T = 293 K
Block, colourless
0.14 × 0.10 × 0.08 mm

Data collection

XtaLAB Synergy, Single source at home/near, HyPix3000 diffractometer
Radiation source: micro-focus sealed X-ray tube, PhotonJet (Cu) X-ray Source
Mirror monochromator
Detector resolution: 10.0000 pixels mm^{-1}
ω scans
Absorption correction: multi-scan (CrysAlisPro; Rigaku OD, 2020)
T_{min} = 0.256, T_{max} = 0.348
3610 measured reflections
1012 independent reflections
915 reflections with $I > 2\sigma(I)$
R_{int} = 0.046
θ_{max} = 71.9°, θ_{min} = 3.7°
h = −14→14
k = −3→4
l = −13→13

Refinement

Refinement on F^2
Least-squares matrix: full
$R[F^2 > 2\sigma(F^2)]$ = 0.056
$wR(F^2)$ = 0.175
S = 1.15
1012 reflections
70 parameters
1 restraint
Hydrogen site location: difference Fourier map
Only H-atom coordinates refined
$w = 1/[\sigma^2(F_o^2) + (0.1175P)^2 + 0.3892P]$ where $P = (F_o^2 + 2F_c^2)/3$
$(\Delta/\sigma)_{max} < 0.001$
$\Delta\rho_{max}$ = 0.95 e Å^{-3}
$\Delta\rho_{min}$ = −0.97 e Å^{-3}

Special details

Geometry. All esds (except the esd in the dihedral angle between two l.s. planes) are estimated using the full covariance matrix. The cell esds are taken into account individually in the estimation of esds in distances, angles and torsion angles; correlations between esds in cell parameters are only used when they are defined by crystal symmetry. An approximate (isotropic) treatment of cell esds is used for estimating esds involving l.s. planes.

Fractional atomic coordinates and isotropic or equivalent isotropic displacement parameters (Å²)

	x	*y*	*z*	U_{iso}*/U_{eq}
Br1	0.08608 (5)	0.68710 (19)	0.36306 (6)	0.0623 (4)
S1	0.22468 (11)	0.3687 (4)	0.58975 (12)	0.0534 (5)
N1	0.3788 (4)	0.2478 (15)	0.4472 (4)	0.0564 (12)
N2	0.2957 (4)	0.4049 (16)	0.3750 (4)	0.0556 (12)
N3	0.4221 (4)	0.069 (2)	0.6501 (5)	0.0641 (15)
H3A	0.484 (5)	−0.02 (2)	0.630 (7)	0.077*
H3B	0.396 (5)	0.05 (2)	0.723 (6)	0.077*
C1	0.3547 (5)	0.2121 (15)	0.5617 (5)	0.0476 (12)
C2	0.2130 (4)	0.4824 (15)	0.4358 (5)	0.0487 (12)

Atomic displacement parameters (Å²)

	U^{11}	U^{22}	U^{33}	U^{12}	U^{13}	U^{23}
Br1	0.0439 (5)	0.0734 (7)	0.0685 (6)	0.0037 (2)	−0.0013 (3)	0.0068 (3)
S1	0.0376 (8)	0.0769 (10)	0.0470 (7)	0.0074 (6)	0.0123 (5)	−0.0004 (6)
N1	0.041 (3)	0.085 (3)	0.044 (2)	0.008 (2)	0.0107 (19)	0.000 (2)
N2	0.042 (2)	0.078 (3)	0.048 (2)	0.002 (2)	0.0105 (18)	−0.001 (2)
N3	0.040 (3)	0.104 (5)	0.050 (2)	0.019 (3)	0.0121 (19)	0.009 (3)
C1	0.035 (3)	0.068 (3)	0.041 (2)	0.002 (2)	0.0104 (19)	−0.003 (2)
C2	0.034 (2)	0.065 (4)	0.047 (2)	−0.003 (2)	0.0013 (18)	−0.005 (2)

Geometric parameters (Å, º)

Br1—C2	1.862 (6)	N2—C2	1.283 (7)
S1—C2	1.732 (6)	N3—C1	1.339 (8)
S1—C1	1.746 (5)	N3—H3A	0.88 (6)
N1—C1	1.311 (6)	N3—H3B	0.88 (6)
N1—N2	1.378 (7)		
C2—S1—C1	86.0 (3)	N1—C1—N3	124.1 (5)
C1—N1—N2	112.6 (4)	N1—C1—S1	113.6 (4)
C2—N2—N1	112.5 (5)	N3—C1—S1	122.3 (4)
C1—N3—H3A	118 (5)	N2—C2—S1	115.4 (4)
C1—N3—H3B	117 (5)	N2—C2—Br1	122.7 (4)
H3A—N3—H3B	124 (7)	S1—C2—Br1	121.9 (3)
C1—N1—N2—C2	0.1 (8)	N1—N2—C2—S1	−0.8 (7)
N2—N1—C1—N3	−179.6 (7)	N1—N2—C2—Br1	−178.3 (4)
N2—N1—C1—S1	0.6 (7)	C1—S1—C2—N2	0.9 (5)

C2—S1—C1—N1	−0.9 (5)	C1—S1—C2—Br1	178.5 (4)
C2—S1—C1—N3	179.3 (7)		

Hydrogen-bond geometry (Å, º)

D—H···*A*	*D*—H	H···*A*	*D*···*A*	*D*—H···*A*
N3—H3*B*···N1^{i}	0.88 (6)	2.60 (7)	3.398 (7)	150 (8)
N3—H3*A*···N1^{ii}	0.88 (6)	2.13 (6)	2.997 (7)	171 (7)
N3—H3*B*···N2^{i}	0.88 (6)	2.14 (6)	2.992 (7)	163 (6)

Symmetry codes: (i) *x*, −*y*+1/2, *z*+1/2; (ii) −*x*+1, −*y*, −*z*+1.